Correlation between atomic ordering and magnetic properties in binary magnetic alloys

Session 1 (June 17-23) : EXAFS analysis of FePtMn system

Participants: S. Laureti (main proposer), N. Safonova, F.D'Acapito

Aim

The aim of this study is to define experimental preparation conditions for the stabilization of the highly anisotropic $L1_0$-chemically ordered FePt phase with addition of a third element (Mn). Manganese is able to affect significantly not only the structural and chemical order, but also the spin configuration due to antiferromagnetic coupling between Mn and Fe moments [Meyer et al., Phys. Rev. B 73 (2006) 214438]. Based on these, Mn is expected to decrease the saturation magnetization as well as increase the ordering parameter while decreasing the annealing temperature for the disordered-ordered transition.

Preliminary analysis of two selected series of samples show that $L1_0$ (001) textured films characterized by high magnetocrystalline anisotropy can be formed after post annealing. The effect of the Mn content and annealing conditions has been studied by X-ray diffractometry and SQUID magnetometry. Selected samples have been characterized by EXAFS and the obtained results are correlated to the magnetic properties.

Experiment Description and Preliminary Analysis

Bi-layered FePt/Mn_x thin films (where Mn concentration *x* corresponds to 0 at.%, 5 at.%, 10 at.%, 15 at.% and 20 at.% of total number of FePt atoms) with total thickness of 5 nm were prepared by dc magnetron sputtering deposition on SiO_2(100 nm)/Si(100) substrates at room temperature. The composition of Fe and Pt in the alloy target, which was used for deposition, is 52% and 48%, respectively. Post-annealing treatments were performed in a Rapid Thermal Annealing (RTA) setup at temperatures of 700°C, 750°C and 800°C for 30 sec, in order to transform the bilayer structure into the $L1_0$ ordered ternary alloy with (001) texture.

Two different series were investigated as summarized in the following tables.

Table 1. Samples with different Mn content, annealed at 750°C:

Sample ID	Total thickness	Mn content at%	T_{ann}
Ch1785 FePt	5 nm	0	750 °C
Ch2050 $FePtMn_{5\ at.\%}$	5 nm	5	750 °C
Ch2051 $FePtMn_{10\ at.\%}$	5 nm	10	750 °C
Ch2052 $FePtMn_{15\ at.\%}$	5 nm	15	750 °C
Ch2053 $FePtMn_{20\ at.\%}$	5 nm	20	750 °C

Table 2. Samples with the same Mn content – 10 at%, annealed at different temperatures:

Sample ID	Total thickness	Mn content at%	T_{ann}
Ch2051 $FePtMn_{10\ at.\%}$	5 nm	10	700 °C
Ch2051 $FePtMn_{10\ at.\%}$	5 nm	10	750 °C
Ch2051 $FePtMn_{10\ at.\%}$	5 nm	10	800 °C

Preliminary characterization: X-ray diffraction (XRD) measurements were performed in order to confirm the presence of desirable (001)-texture and $L1_0$ ordering. For the magnetic characterization, superconducting quantum interference device - vibrating sample magnetometry (SQUID-VSM) with magnetic fields up to 70 kOe was carried out at room temperature. Resulting hysteresis loops (not shown) confirm that prepared samples possess an out-of-plane easy axis of magnetization. Nevertheless, a hysteresis with a non-zero remanence for in-plane geometry is still present consistent with the presence of the (111) reflection in XRD. Furthermore a significant decrease in magnetization was observed with increase of Mn concentration (40 - 60% compare to $L1_0$-FePt), which suggests the presence of antiparallel coupling between Fe and Mn moments.

EXAFS characterization: XAS data collection was carried out at the Mn-K_α (6539 eV), Fe-K_α (7112 eV), and Pt-L_{III} (11564 eV) edges with the polarization vector of the X-ray beam being either *parallel* or *perpendicular* to the sample surface in order to enhance the sensitivity to differently oriented bonds for the two cases. This approach provides more detailed description of the anisotropic distribution of atoms within the alloy. The angle between the X-ray polarization vector and the normal to the surface was 75° in *parallel* and 15° in *perpendicular* configuration, and this latter condition permitted also the minimization of the coherent scattering signal from the Si

substrate and to enhance the fluorescence from the atoms under study. During data collection, the samples were kept at a temperature of 100 K to reduce the thermal atomic vibrations thus enhancing the EXAFS signal. The absorption coefficient was measured via the fluorescence yield from Mn-K_α, Fe-K_α and Pt-L_{III} lines using an energy-resolving (12)-elements high purity germanium detector (energy resolution of about 250 eV). XAS data extraction and fitting was carried out with the ATHENA and ARTEMIS codes (Ravel & Newville, J. Synchrotron Rad. 12 (2005) 537) while quantitative modelling was based on simulated EXAFS signals using the FEFF8.1 code (Ankudinov et al., Phys. Rev. B 58 (1998) 7565).

Although the full analysis of all the data acquired at the Mn-K, Fe-K and Pt-L_{III} edges for the two series of samples is still in progress, the preliminary analysis revealed fundamental aspects related to the deposition process which will be taken into account for the future experiments. In particular, the study is aimed at determining the role of the Mn atoms in FePtMn $L1_0$ alloys on the magnetic properties, being the latter strongly dependent on the chemical and structural properties and, in particular, on the chemical ordering. The analysis at the Pt edge, carried out by fitting the data with a substitutional model developed for a similar system (FePtCu, Laureti et al. J. Applied Crystallography, 47 (2014) 1722), **(fig. 1, 2, 3, table 3)** revealed a fraction of the ordered $L1_0$ phase that is not significantly affected by the presence of the Mn third element differently to what previously observed for FePtCu. Such a result is consistent with the analysis of the Mn-K_α data, which showed that a significant amount of Mn is not included into the alloy, being surrounded by oxygen atoms to form a Mn_xO_y stable phase. However, a preliminary magnetic characterization carried out by SQUID-VSM revealed a strong magnetic anisotropy which was attributed to a high ordering degree, that is actually not supported by the EXAFS analysis carried out with such a model, which gives values for the X ordering parameter below 0.4 (i.e. only 40% of ordered phase). Such a discrepancy may be attributed to the presence, in some samples, of a significant fraction of (111) oriented grains; in other words, the coexistence of the (100) and (111) growth directions may affect the EXAFS spectra being the atomic arrangement around the absorber atom in the parallel and perpendicular configuration different for the two orientations.
On the basis of these preliminary results we are currently developing a new model which is able to account for the different Pt-Pt and Pt-Fe in plane and out of plane distances in the two orientations. The comparison between the two models applied at the Pt, Mn and Fe edges is still under progress.

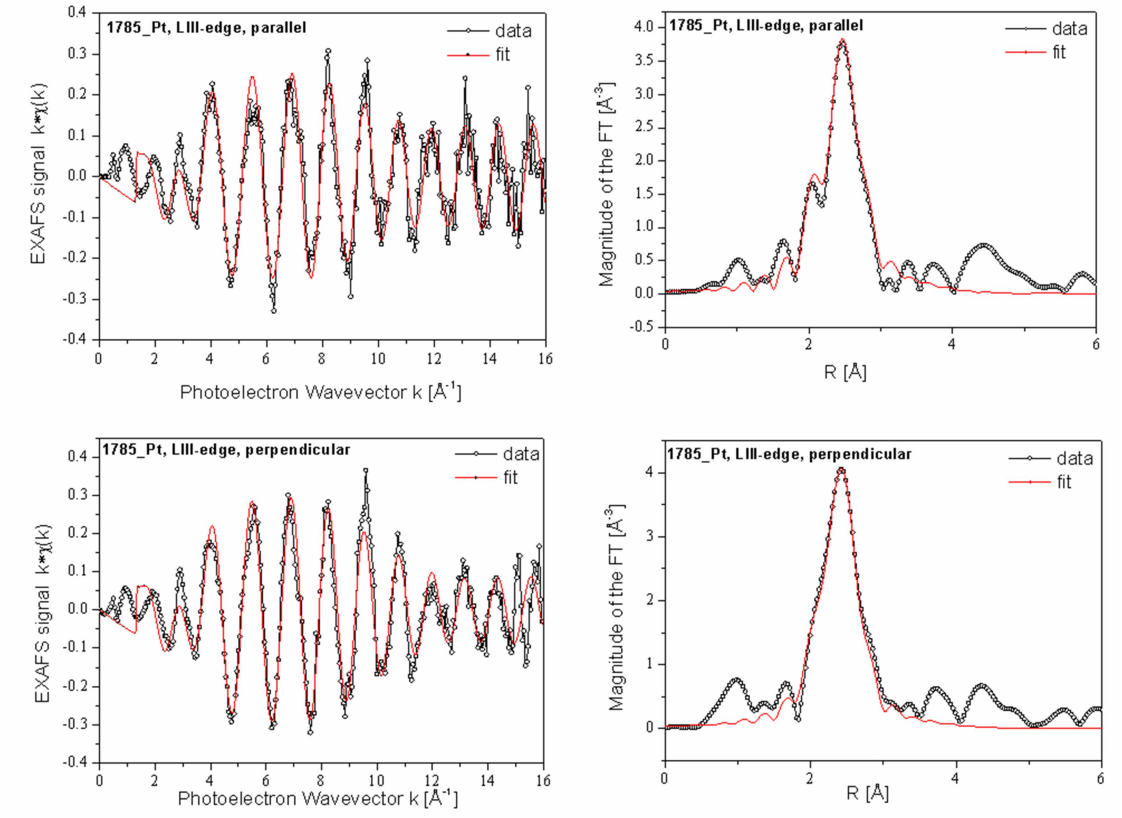

Figure 1 – XAS spectra taken at the Pt-L_{III} edge (parallel and perpendicular polarizations) for sample Ch1785 FePt and corresponding Fourier transform are shown. In addition, simulation results (first shell analysis) are included.

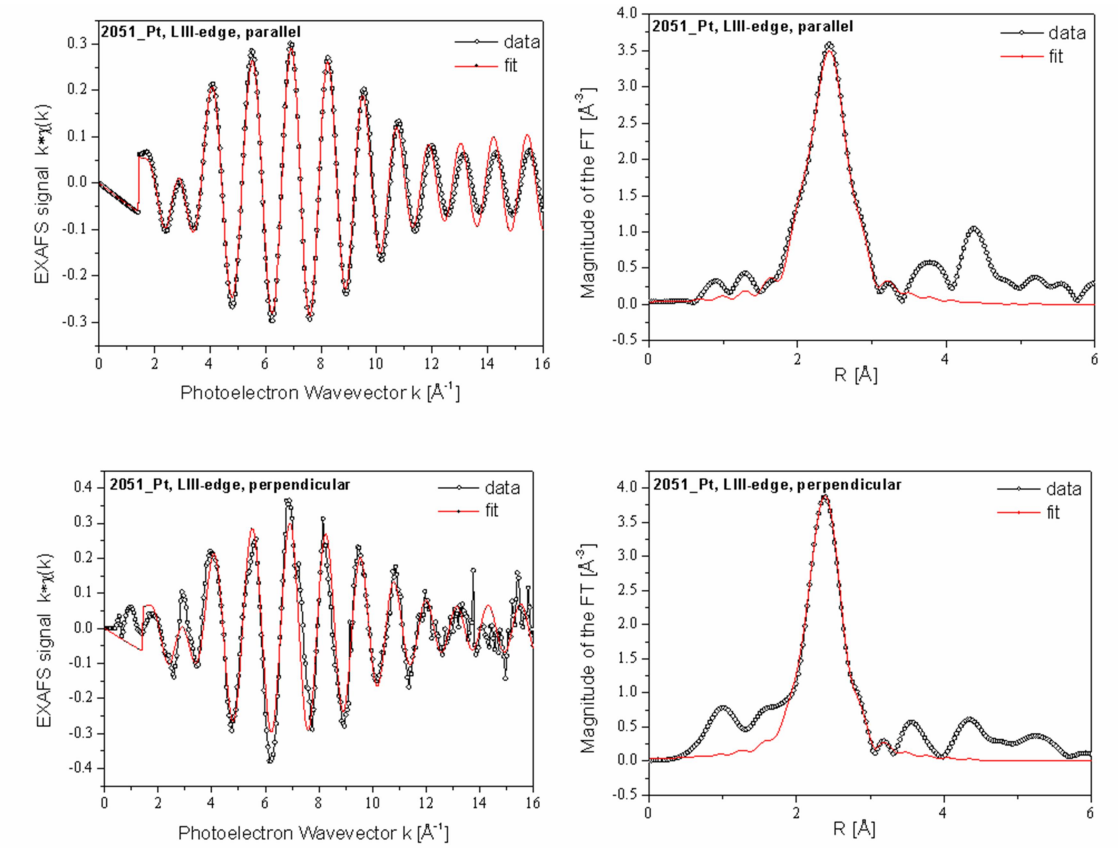

Figure 2 – XAS spectra taken at the Pt-L_{III} edge (parallel and perpendicular polarizations) for sample Ch2051 $FePtMn_{10\ at.\%}$ and corresponding Fourier transform are shown. In addition, simulation results (first shell analysis) are included.

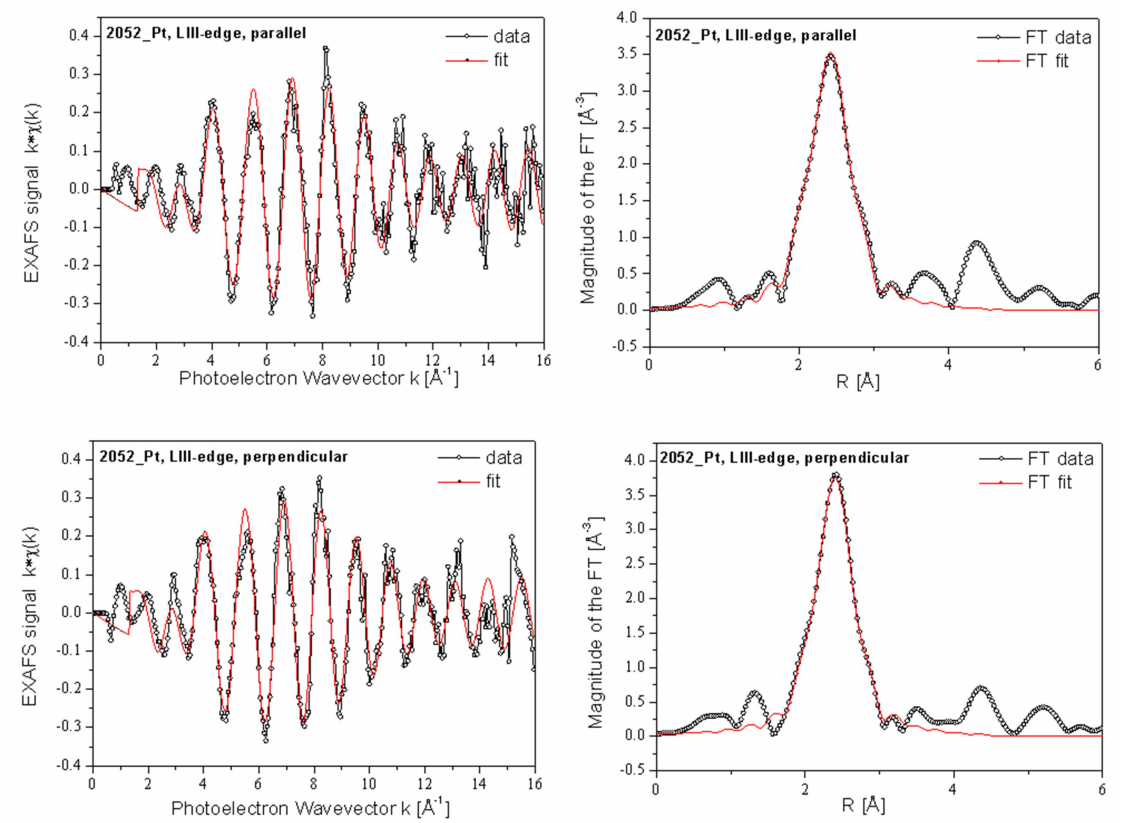

Figure 3 – XAS spectra taken at the Pt-L_{III} edge (parallel and perpendicular polarizations) for sample Ch2052 $FePtMn_{15\ at.\%}$ and corresponding Fourier transform are shown. In addition, simulation results (first shell analysis) are included.

Table 3 – Fitting parameters for samples Ch1785 FePt, Ch2051 $FePtMn_{10at.\%}$, and Ch2052 $FePtMn_{15at.\%}$.

sample ID	**amp**	**E_0**	**X**	**DIRECT**		**INVERSE**	
				Pt-Fe dir	**Pt-Pt dir**	**Pt-Pt inv**	**Pt-Fe inv**
				th: 2.6948 Å	*th:2.7577 Å*	*th: 2.6948 Å*	*th: 2.7577 Å*
Ch1785 FePt	0.92±0.06	7±1	0.3±0.1	2.658±0.009	2.72±0.02	2.71±0.01	2.74±0.04
Ch2051 $FePtMn_{10\ at.\%}$	0.88±0.03	7.6±0.9	0.39±0.09	2.66±0.007	2.74±0.01	2.72±0.01	2.68±0.03
Ch2052 $FePtMn_{15\ at.\%}$.	0.9±0.02	6.8±0.7	0.19±0.07	2.659±0.005	2.739±0.007	2.719±0.005	2.67±0.01

Session 2 (November 18-23) : EXAFS study of the chemical and structural evolution of $L1_0$ FePt alloy directly synthesized from $FePtCl_6 \cdot 6H_2O$ precursor

Participants: S. Laureti (main proposer), A. Capobianchi, E. Patrizi, A. Puri, F. D'Acapito

Aim

The experiment was aimed at studying the structural and atomic evolution of the $FePtCl_6 \cdot 6H_2O$ salt during its transformation, during annealing, to the chemically ordered FePt $L1_0$ alloy. Generally, FePt nanoparticles are obtained in the chemically disordered fcc phase, and a post-growth annealing treatment at about 600°C is necessary to induce the transition to the chemically ordered fct phase ($L1_0$). The high annealing temperature of this process possesses noticeable drawbacks like particle coalescence phenomena with the consequent increase of the particle size, size dispersion, and reduction of the magnetic anisotropy. Recently, a new chemical strategy has been reported, aimed at obtaining the direct synthesis of $L1_0$ FePt alloy nanoparticles starting from a polycrystalline molecular compound, the iron (II) chloroplatinate hexahydrate ($FePtCl_6 \cdot 6H_2O$), in which Fe and Pt atoms are arranged on alternating planes (fig.1) like in the fct FePt structure [A.Capobianchi, M. Colapietro,D. Fiorani, S. Foglia, P. Imperatori, S.Laureti, E. Palange *Chemistry of Materials* 21 (2009) 2007; A. Capobianchi, G. Campi, M. Camalli, C. Veroli, *Z. Kristallogr*. 224 (2009) 384–388].

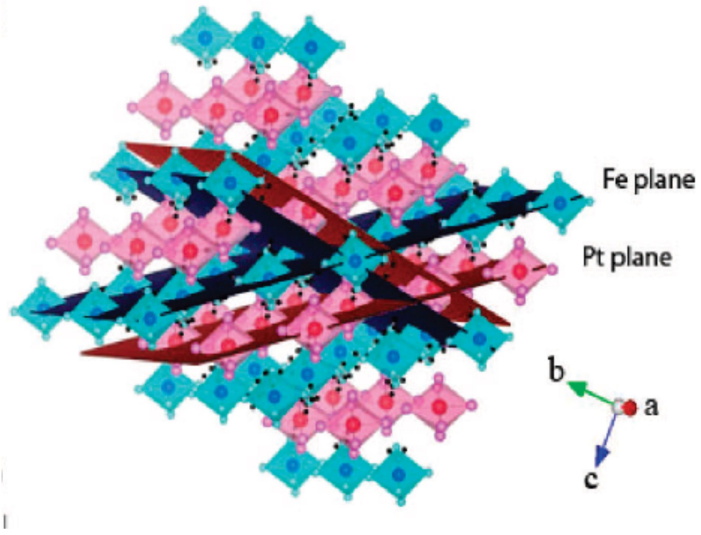

Fig. 1 $FePtCl_6 \cdot 6H_2O$ crystal packing showing the alternating Fe and Pt atomic planes

The reduction of such compound by 5% H_2 and 95% Ar at a reduced temperature (400°C) leads directly to a highly ordered $L1_0$ phase. From a thermodynamic point of view, the peculiar Fe-Pt atomic arrangement on alternating planes, as in the crystalline structure of $FePtCl_6 \cdot 6H_2O$, represents the driving force for the direct formation of the fct FePt alloy during the heating process; thus, the crystalline structure of $FePtCl_6 \cdot 6H_2O$ used for the synthesis acts as a precursor to directly obtain the chemically ordered $L1_0$ FePt phase. In order to follow the thermal evolution of the system, in a previous work the heating process of the $FePtCl_6 \cdot 6H_2O$ powder under reductive atmosphere was monitored by a thermogravimetric and differential thermal analysis (TGA-DTA) (Fig. 2) but it was not possible to isolate and characterize each single step, the processes being partially overlapped.

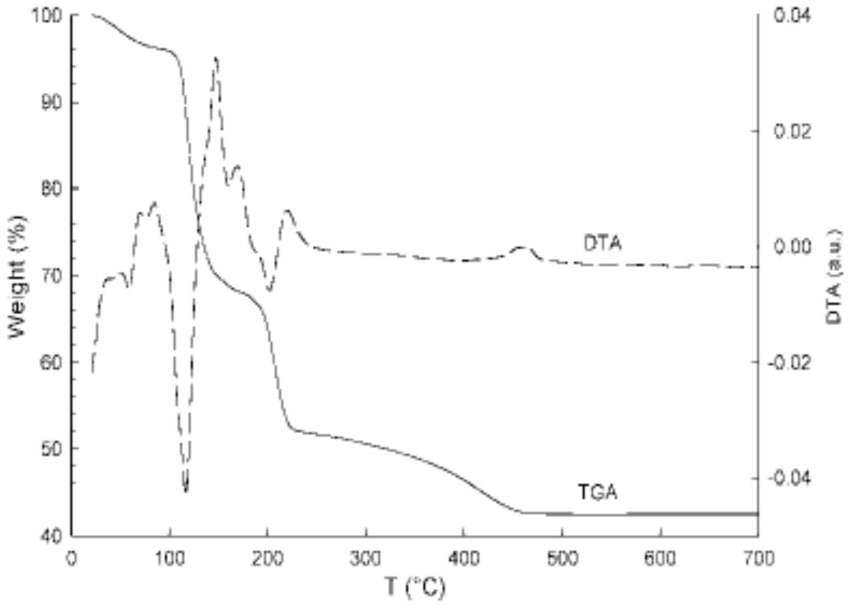

Fig. 2 TGA-DTA of FePtCl6 ·6H2O under flux of 95% Ar and 5% H_2

A combination of *ex-situ* and *in situ* XAS experiments have been carried out at the Pt-L_{III} and Fe-K_α edges with the aim of describing the local environment around the metals during the thermal reduction of the precursor salt and to elucidate the mechanism at the basis of such structural evolution.

Experiment Description and Preliminary Analysis

The powder of the crystalline precursor salt $FePtCl_6 \cdot 6H_2O$ has been previously prepared in our home laboratory according to the synthesis proposed in [A.Capobianchi, M. Colapietro, D. Fiorani, S. Foglia, P. Imperatori, S.Laureti, E. Palange *Chemistry of Materials* 21 (2009) 2007]. The initial and final phases together with different samples taken at intermediate steps of the annealing treatment have been prepared by heating the precursor salt at 5°C/min under a reductive H_2/Ar atmosphere and stopping the process at 200°C, 300°C and 400°C. For these stages, the preliminary structural (XRD) and magnetic (SQUID and VSM) characterizations gave evidence of a magnetically soft FePt fcc structure (i.e. chemically disordered phase) which is actually not expected as an intermediate structure between two (initial and final) ordered crystallographic phases.

The XAS experiment consisted in two parts:

ex-situ analysis:

The local structural evolution during the treatment has been studied by EXAFS carried out on the powder samples prepared in the home laboratory at the Fe-K and Pt-L_{III}, edges in transmission mode, in order to obtain a description of the local environment around these metals in the initial crystal, during the treatment (i.e. in samples annealed at intermediate temperature) and in the final product.

in-situ analysis:

Samples of $FePtCl_6 \cdot 6H_2O$ crystalline film has been put into a heating cell designed for *in-situ* X-ray absorption experiments at high temperature and under a reactive atmosphere (fig. 3).

Fig. 3 Microtomo Furnace [http://www.esrf.eu/home/UsersAndScience/Experiments/SciInfra/SampleEnvironment/high-temperature/microtomo-furnace.html].

Before the in-situ experiment the furnace conditions (5°C/min temperature ramp; H_2/Ar gas flow) have been carefully set in order to ensure the process reproducibility, which has been tested by comparing the EXAFS spectra of the sample after treatment with the ex-situ spectra of a FePt $L1_0$ sample obtained in the home furnace.

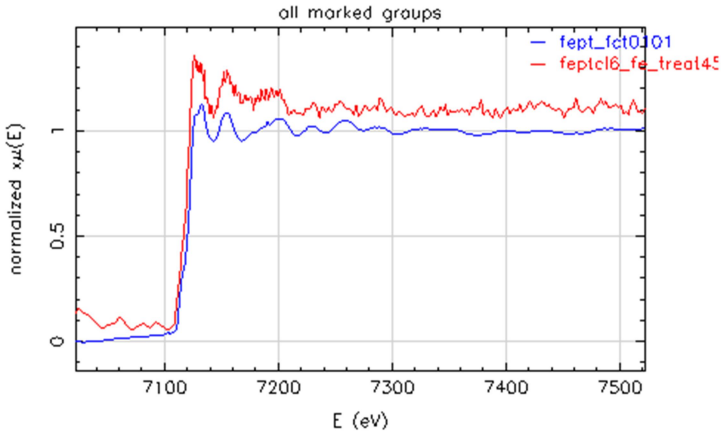

Fig. 3 Comparison between EXAFS spectrum at the Fe-Ka edge for the pure FePt alloy obtained at the home laboratories (blu) and the FePt alloy after the in-situ treatment of the FePtCl6 salt (red). Please, note that the red curve has been obtained by measuring the sample at 450°C

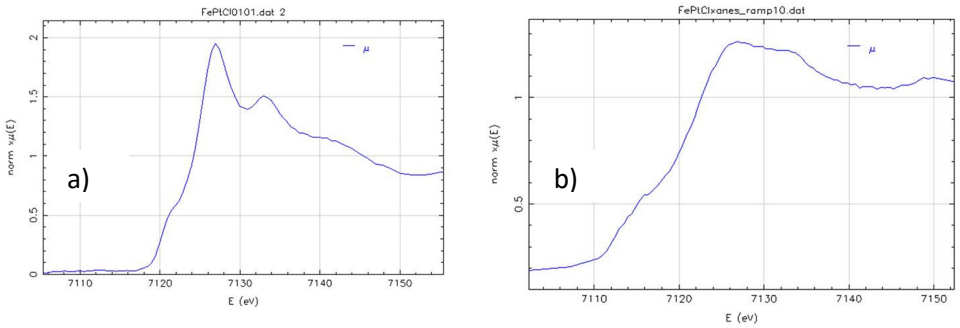

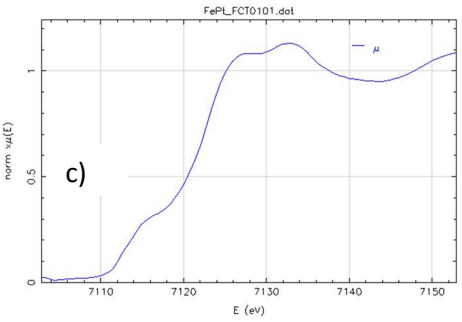

Fig. 4 Comparison between XANES spectra at the Fe-Ka edge for the $FePtCl_6$·H2O sample before the treatment (a) after the in-situ treatment (b) and for the FePt alloy obtained after the $FePtCl_6$·H2O treatment in the home laboratories (c).

The annealing has been performed by heating the sample at 400 °C with a rate of 5 °C/min, under H_2/Ar reductive atmosphere. Quick-XANES spectra have been collected at the Fe-Kα and $Pt\text{-}L_{III}$ edge in transmission mode, during two separated processes to follow the chemical/structural evolution around the two elements during the treatment. Spectra of 4s/each have been collected at a rate of 3 spectra/minute every 10 °C of the heating process. The same apparatus has been also used to carry out static EXAFS experiments in stationary temperature conditions (i.e. EXAFS spectra acquired at defined temperatures of the heating treatment). In fig. 5 the comparison between different quick-XANES spectra collected during the treatment at the Fe-K edge highlights the clear evolution of the chemical environment and electronic state of the absorber atoms.

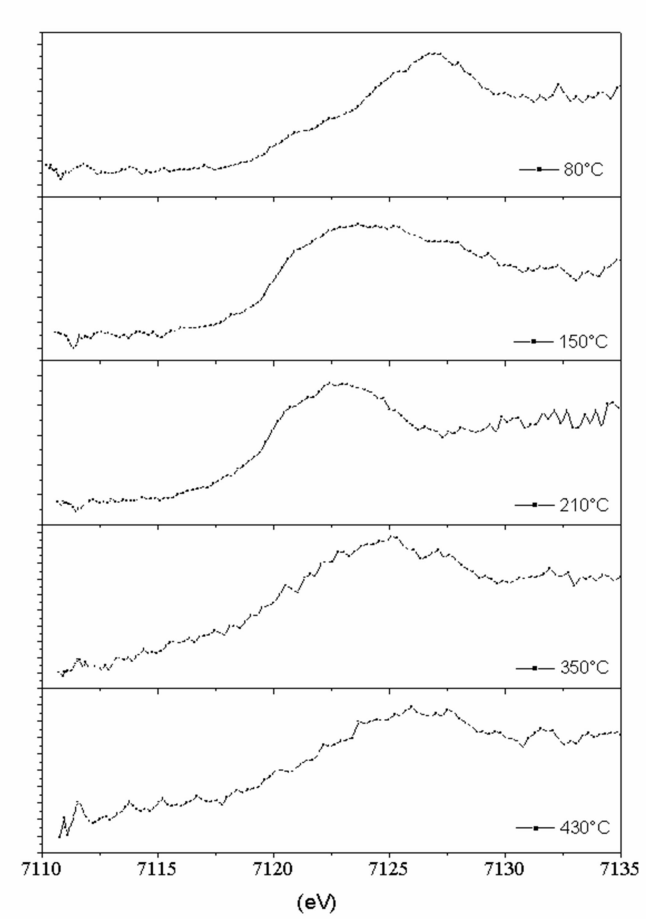

Fig. 5 Comparison between quick-XANES spectra at the Fe-K_α edge for the $FePtCl_6 \cdot H_2O$ sample during the annealing treatment.

Session 3 (April 12-19) : The IrMn/NiFe exchange coupled bilayer: a structural and chemical analysis by EXAFS

Participants: S. Laureti (main proposer), F. Spizzo, G. O. Lepore, F. D'Acapito

Aim

The third session was aimed at studying a peculiar magnetic system characterized the exchange coupling at the interface between an antiferromagnetic (AFM) and a ferromagnetic phase (FM). Such a system is widely used in magnetoresistive devices where the magnetization direction of the FM reference layer is stabilized through the exchange interaction at the FM/AF interface (Exchange Bias (EB) phenomenon). Up to now, the best performance in terms of EB strength has been found in systems with the IrMn alloy as AFM. Actually, for the $IrMn_3$ composition, two different phases have been observed: a chemically disordered face-centered cubic structure (γ-$IrMn_3$), and a chemically ordered $L1_2$ phase, where planes of Mn atoms and mixed Ir and Mn atoms alternate along the 001 direction, without affecting however, the lattice parameters (i.e. c/a ratio). Although the magnetic anisotropy of the disordered phase ensures a large EB field and thermal stability suitable for application, in a recent paper [A. Kohn, Sci. Rep., 2013, DOI: 10.1038/srep02412], a significant variation in the magnetization reversal mechanism and in the EB field has been experimentally demonstrated when the FM layer is exchange coupled to the chemical ordered $L1_2$-$IrMn_3$ phase. The amount of $L1_2$ phase, that positively affects the EB strength at the AF/FM interface, is generally influenced by the buffer layer used for the $Ir_{25}Mn_{75}$ alloy deposition. However, recent experiments have shown that the strength of the coupling is also increased by thermal annealing. The aim of this experiment was to elucidate the effect of different buffer layer (Cu or NiFe) and of the thermal effects (deposition temperature or post-deposition thermal annealing) on the structural and chemical order and, consequently, to correlate it to the observed magnetic properties. Moreover, the presence of a very thin Cu intra-layer at the FM/AFM interface resulted in a further modulation of the exchange bias effect. In this experiment, the high sensitivity of the technique has been used to investigate the atomic arrangement around the Cu atoms in a $Ir_{25}Mn_{75}$/Cu (0.2 nm) /$Ni_{80}Fe_{20}$ sample.

This activity is part of a national project (FIRB-2012-1016, Project Coordinator: S. Laureti; Unit responsible: F. Spizzo) titled "NANOREST- Tailoring the magnetic anisotropy of nanostructures for enhancing the magnetic stability of magnetoresistive junctions", which includes the study of arrays

of sub-50 nm perpendicular spin valves in which each electrode consists of $Ir_{25}Mn_{75}/Ni_{80}Fe_{20}$ exchange coupled phases prepared by sputtering.

Experiment Description and Preliminary Analysis

The samples deposition process was carried out by dc-magnetron sputtering in a 0.5 Pa Ar atmosphere at room temperature and in the presence of a static magnetic field, H_{dep} =400 Oe. The atomic composition of the AFM and FM targets was $Ir_{25}Mn_{75}$ and $Ni_{80}Fe_{20}$, respectively. In the following table the list of the samples with the relative stacking order is reported (in parentheses the nominal thickness of each layer as determined after calibrating the sputtering sources with a quartz microbalance).

Sample					
IrMn125H	Si	NiFe (5 nm)	IrMn (10 nm)	\	NiFe (5 nm)
IrMn126H	Si	NiFe (5 nm)	IrMn (10 nm)	Cu (0.1 nm)	NiFe (5 nm)
IrMn131H	Si	NiFe (5 nm)	IrMn (10 nm)	Cu (0.2 nm)	NiFe (5 nm)
IrMn128H	Si	Cu (5 nm)	IrMn (10 nm)	\	NiFe (5 nm)
IrMn145H	Si	Cu (5 nm)	NiFe (5 nm)	IrMn (10 nm)	Cu (5 nm)
IrMn146H	Si	Cu (5 nm)	IrMn (10 nm)	\	NiFe (5 nm)
IrMn146H / TT400K@3T	Si	Cu (5 nm)	IrMn (10 nm)	\	NiFe (5 nm)
IrMn147 / with H appl	Si	Cu (5 nm)	IrMn (10 nm)	\	NiFe (5 nm)

For all samples XAS data collection was carried out at the Ir-L_{III} (11215 eV), Mn-K_α (6539 eV), edges with the angle between the X-ray polarization vector and the normal to the surface of 75° in *parallel* and 10° in *perpendicular* configuration while additional measurements on selected samples have been carried out at the Ni-K_α (8339 eV), and Cu- K_α (8993 eV), with an angle of 45°. During data collection, the samples were kept at a temperature of 80 K to reduce the thermal atomic vibrations thus enhancing the EXAFS signal. The absorption coefficient was measured via the fluorescence yield using an energy-resolving (12)-elements high purity germanium detector (energy resolution of about 250 eV).

Due to the recent data acquisition, the current activity is related to the data processing and comparison among signals acquired at the Ir-L_{III} edge on different samples in different conditions.

In particular, such preliminary step is aimed at determine the existence of a difference between the signal acquired in parallel and perpendicular configuration for identifying, in addition to the structural ordering, the possible chemical ordering in the IrMn alloy. Indeed, the preliminary magnetic characterization revealed significant differences among samples in term of strength of the exchange coupling (i.e. in the horizontal displacement of the field cooling hysteresis loop) which is related to the nature of the AFM layer and on the microstructural properties of the interface. For this reason, since the chemical and structural properties of the AFM IrMn alloy is expected to be affected by the nature of the buffer layer and by the deposition conditions, the preliminary analysis has been devoted at analysing the parallel and perpendicular signals of 4 samples:

IrMn125H Si/NiFe/IrMn/NiFe (with NiFe as underlayer)
IrMN128H Si/Cu/IrMn/NiFe (with Cu as underlayer)
IrMn146TT Si/Cu/IrMn/NiFe (post-dep annealed at 400°K under $\mu_0 H_{appl}$=3T)
IrMn147 Si/Cu/IrMn/NiFe (deposited under $\mu_0 H_{appl}$ =0.4 T)

In all cases the absorption spectra acquired in parallel and perpendicular configuration resulted perfectly superimposed (fig. 6) indicating a quite isotropic atomic distribution within the alloy.

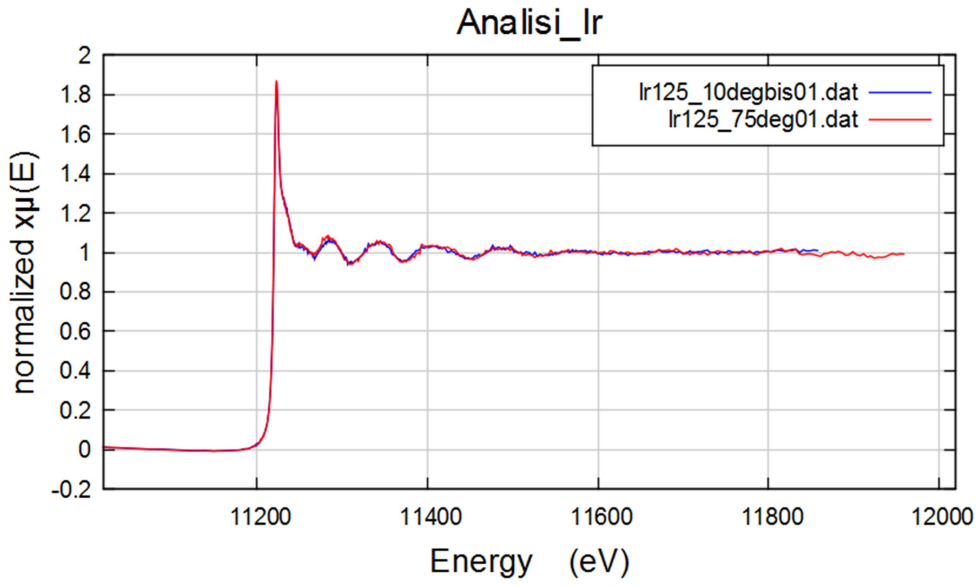

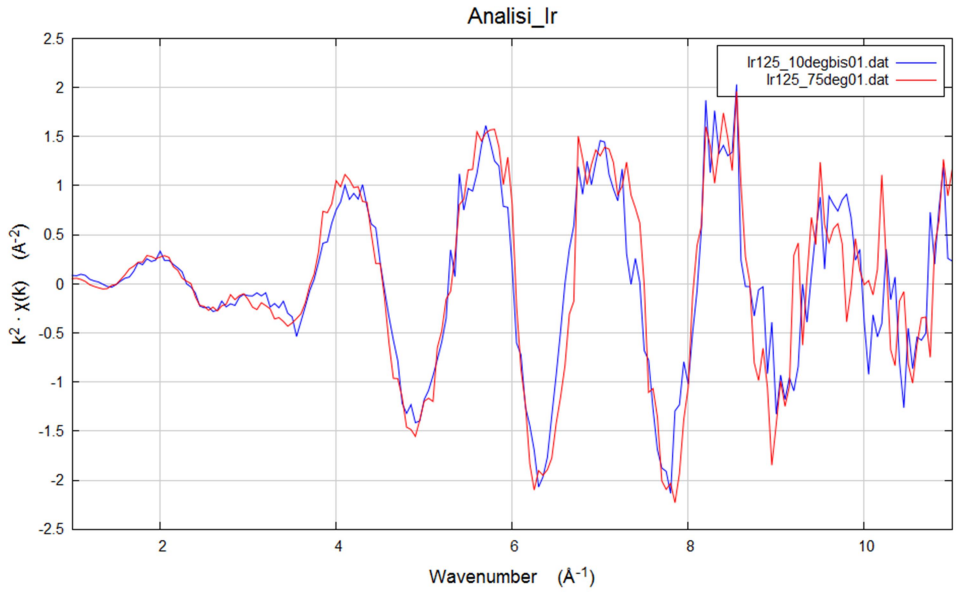

Fig. 6 Comparison between EXAFS spectra (μ(E), upper and $k^2\chi(k)$, lower) at the Ir-L_{III} edge for sample IrMn125H

Moreover, the different buffer layer and post-deposition conditions seem do not significantly affect the structural and chemical ordering of the IrMn alloy, although the magnetic properties resulted clearly altered. In fig. 7 the EXAFS signal and the relative Fourier Transform for different samples are reported.

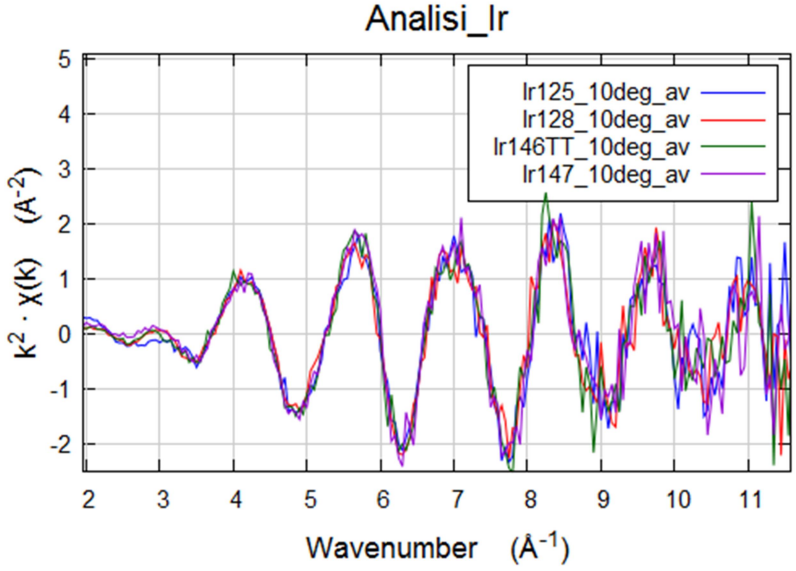

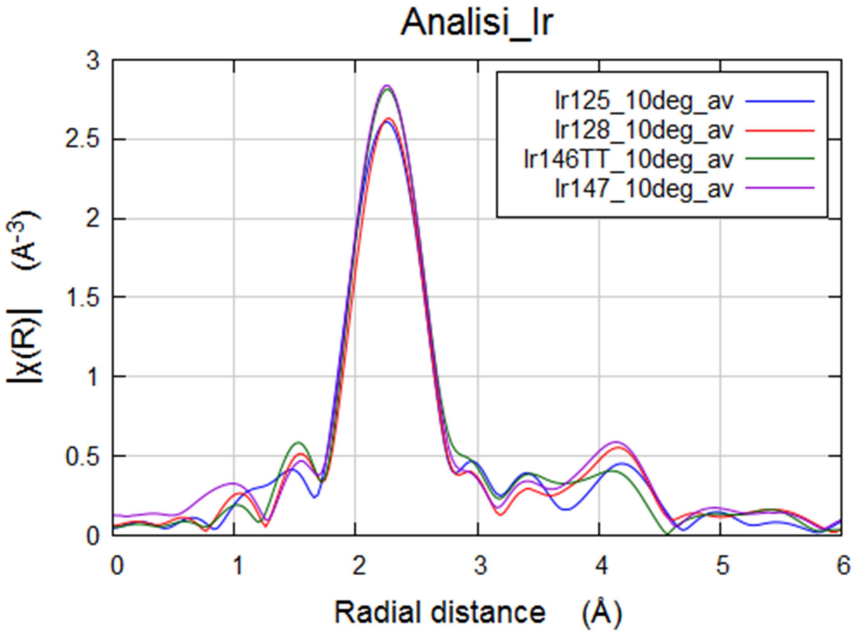

Fig. 7 Comparison between EXAFS spectra, $k^2\chi(k)$ (upper) and the relative FT (lower) at the Ir-L_{III} edges

In other words, the significant difference in the magnetic behaviour (as evidenced in fig. 8) cannot be ascribed to differences in the chemical or structural order of the IrMn layer, but is strictly related to the magnetic order at the interface. The analysis of samples with the inclusion of Cu atoms at the interface will be fundamental in confirming such effect.

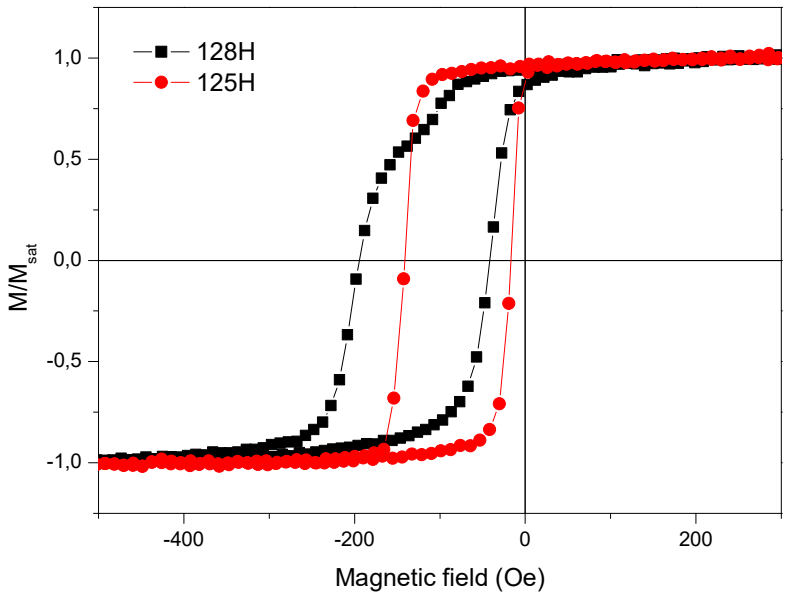

Fig. 8 Room temperature hysteresis loops of samples 128H and 125H